

Northern Indian Ocean Salt Transport (NIOST): Estimation of Fresh and Salt Water Transports in the Indian Ocean using Remote Sensing, Hydrographic Observations and HYCOM Simulations

PI: Dr. Subrahmanyam Bulusu
Department of Earth and Ocean Sciences
University of South Carolina
Columbia, SC 29208
phone: (803) 777-2572 fax: (803) 777-6610 email: sbulusu@geol.sc.edu

Award Number: N00014-12-1-0454

LONG-TERM GOALS

Sea surface salinity (SSS) variability contributes to variability of the global hydrologic cycle and oceanic processes such as circulation and heat storage. Salinity and temperature together affect the density of seawater and thus its circulation. Though water temperature and SST have been measured extensively by in-situ observations and remote sensing, extensive salinity observations have been lacking. The launch of the European Space Agency's SMOS satellite on November 2, 2009, and NASA and Space Agency of Argentina's (Comision Nacional de Actividades Espaciales, CONAE) Aquarius/SAC-D satellite mission in June 10, 2011 opened a new era by providing global salinity observations, which will improve our understanding of salinity variability and dynamics. Part of our motivation for this work is to provide a future reference for Indian Ocean salt flux computed with data from the SMOS and Aquarius salinity satellite missions, fresh and salt water transports and budget using HYCOM simulations and Hydrographic observations.

Horizontal surface salt flux in the Indian Ocean is important because it affects air-sea interactions on different time scales. Such processes are not entirely understood, especially on long time scales, due to a paucity of salinity observations. The use of model output to estimate second-order oceanic properties such as flux and transport can be challenging because although models do well simulating primary properties such as velocity and salinity, the integration of these primary variables do not have the same level of desired accuracy. Nevertheless, model output has been used to estimate ocean volume and salt flux and transports to a fairly good degree of agreement with observational data.

In this project we showed the dominant spatial and temporal patterns of near-surface salt flux variability, fresh and saltwater transports in the Indian Ocean. We also addressed the impacts that IOD and ENSO have on salt flux.

OBJECTIVES

1. To estimate near surface salt transport using satellite and *in situ* salinity observations and compare with HYCOM simulated near surface salinity fields, and obtain depth- integrated salt transport from HYCOM.

Report Documentation Page				Form Approved OMB No. 0704-0188	
Public reporting burden for the collection of information is estimated to average 1 hour per response, including the time for reviewing instructions, searching existing data sources, gathering and maintaining the data needed, and completing and reviewing the collection of information. Send comments regarding this burden estimate or any other aspect of this collection of information, including suggestions for reducing this burden, to Washington Headquarters Services, Directorate for Information Operations and Reports, 1215 Jefferson Davis Highway, Suite 1204, Arlington VA 22202-4302. Respondents should be aware that notwithstanding any other provision of law, no person shall be subject to a penalty for failing to comply with a collection of information if it does not display a currently valid OMB control number.					
1. REPORT DATE 30 SEP 2013		2. REPORT TYPE		3. DATES COVERED 00-00-2013 to 00-00-2013	
4. TITLE AND SUBTITLE Northern Indian Ocean Salt Transport (NIOST): Estimation of Fresh and Salt Water Transports in the Indian Ocean using Remote Sensing, Hydrographic Observations and HYCOM Simulations				5a. CONTRACT NUMBER	
				5b. GRANT NUMBER	
				5c. PROGRAM ELEMENT NUMBER	
6. AUTHOR(S)				5d. PROJECT NUMBER	
				5e. TASK NUMBER	
				5f. WORK UNIT NUMBER	
7. PERFORMING ORGANIZATION NAME(S) AND ADDRESS(ES) University of South Carolina, Department of Earth and Ocean Sciences, Columbia, SC, 29208				8. PERFORMING ORGANIZATION REPORT NUMBER	
9. SPONSORING/MONITORING AGENCY NAME(S) AND ADDRESS(ES)				10. SPONSOR/MONITOR'S ACRONYM(S)	
				11. SPONSOR/MONITOR'S REPORT NUMBER(S)	
12. DISTRIBUTION/AVAILABILITY STATEMENT Approved for public release; distribution unlimited					
13. SUPPLEMENTARY NOTES					
14. ABSTRACT					
15. SUBJECT TERMS					
16. SECURITY CLASSIFICATION OF:			17. LIMITATION OF ABSTRACT Same as Report (SAR)	18. NUMBER OF PAGES 12	19a. NAME OF RESPONSIBLE PERSON
a. REPORT unclassified	b. ABSTRACT unclassified	c. THIS PAGE unclassified			

2. To address the salinity variability at intraseasonal, interannual and decadal time scales and its impact on the circulation and particularly the coastal currents.
3. To study of role of salinity on the barrier layer dynamics in the Bay of Bengal (BoB), Arabian Sea (AS) and Equatorial Indian Ocean (EIO).
4. To study the role of the coastal Kelvin waves on the fresh and salt water transports.

APPROACH

WORK COMPLETED

1. Variability of Salt flux in the Indian Ocean during 1960-2008

In this study we studied near-surface horizontal salt flux in the Indian Ocean during 1960-2008 using the Simple Ocean Data Assimilation (SODA) Reanalysis version 2.2.4. The long term mean salt flux showed seasonal reversals that are more pronounced in the northern Indian Ocean than in the southern Indian Ocean. Mean zonal salt flux is of a higher magnitude than the mean meridional salt flux. Wyrski jets influence zonal salt flux in the equatorial region. Meridional salt flux is northward along the northeast African coast and western Bay of Bengal (BoB) during the southwest monsoon (SW) season. The opposite holds during the northeast (NE) monsoon season. Empirical Orthogonal Function (EOF) analyses of salt flux showed that the Indian Ocean Dipole (IOD) primarily controls interannual variability with flux being westward during positive dipole events and eastward during negative dipole events. The co-occurrence of IOD with the El Niño Southern Ocean (ENSO) results in enhanced salt flux especially along the equatorial region. Spatially, the most variable regions are the northeast African coast, eastern Arabian Sea (AS), BoB and equatorial regions. This study will help interpret salinity data for the Indian Ocean from the recently launched Soil Moisture Ocean Salinity (SMOS) and Aquarius satellite salinity missions.

2. Role of Coastal Kelvin Waves in the Bay of Bengal circulation

Kelvin waves originating in the equatorial Indian Ocean propagate along the equatorial wave-guide until reaching the Sumatra coast and follow the coastal waveguide counter clockwise around the perimeter of the Bay of Bengal (BoB). We observed these Kelvin waves using sea surface height (SSH) anomalies derived from satellite altimeter observations for the 1993-2006 period, the Simple Ocean Data Assimilation (SODA) reanalysis for the 1993-2006 period and the HYbrid Coordinate Ocean Model (HYCOM) simulations for the 2002-2006 period. Wavelet analyses of each time series of SSH data at five selected locations revealed a dominant annual period in the equatorial Indian Ocean, progressing to a semiannual period off the Sumatra coast, and transitions into both annual and 120-day period around the perimeter of the BoB and along the east coast of India. In this study, we discuss the variability in the propagation of the upwelling Kelvin waves during the winter monsoon (January-March) and summer monsoon (July-September) and the downwelling Kelvin waves during the summer monsoon transition (April-June) and winter monsoon transition (October-December) and the associated variability in the surface circulation in the study area from each data set. The winter transition downwelling Kelvin wave showed progressive propagation all along the equatorial region, coastal BoB and along the west coast of India to its northern edge, thus affecting India's coastal circulation. Under its influence, the equatorward flowing East India Coastal Current (EICC) and the poleward flowing West India Coastal Current (WICC) with an embedded Lakshadweep High

(anticyclonic eddy) in the southeastern Arabian Sea are well developed. We studied the role of these coastal Kelvin waves on fresh and salt water transports in the Indian Ocean.

3. SMOS Mission reveals salinity structure of the Indian Ocean Dipole

This study reports the first European Space Agency's (ESA) Soil Moisture and Ocean Salinity (SMOS) observations of the sea surface salinity (SSS) structure during an Indian Ocean dipole (IOD) event. Comparisons with Argo data show that the SMOS satellite is able to resolve the observed SSS pattern in the Indian Ocean with some challenges in the northern Indian Ocean. Results of box-averages for the Java Sumatra Coast (JSC) and South Central Indian Ocean (SCIO) regions show anomalously low SSS in the former and anomalously high SSS in the latter during the 2010 negative IOD event. Analyses of salt flux and salt budget terms suggest that in the JSC region the salt tendency is an interplay between the freshwater forcing and horizontal advection terms with increased precipitation having a higher impact in driving anomalous SSS than advection. In the SCIO region, advection seems to be more important than the freshwater forcing term.

RESULTS

1. Long-term mean Salt Flux in the Indian Ocean

The long-term monthly means of near-surface meridional salt flux in the Indian Ocean are shown in Figure 1. A seasonal reversal of flux is more pronounced in the northern Indian Ocean than the southern Indian Ocean with well defined regions being the western Bay of Bengal (BoB), eastern Arabian Sea (AS) and the East African Coastal Current (EACC)/Somali Current (SC). SSS flux along the eastern Agulhas Current, Madagascar and the Leeuwin Current regions do not clearly exhibit a seasonal reversal, instead flux is southward throughout the year. During the spring inter-monsoon (Figure 1a), salt flux is northward along the western BoB and the SC region. The flux along the western BoB is under the influence of the East Indian Coastal Current (EICC) which reverses direction twice in a year, flowing northeastward between February and September with a peak in March-April. During AM (Figure 1a), northward flux along the SC region is enhanced with a greater spatial spread than during the NE monsoon (Figure 1d). During the SW monsoon (Figure 1b), northward salt flux along the SC region is well established whereas the northward flux observed during AM along the western BoB begins to diminish in magnitude. During this time the entire central and eastern AS is dominated by southward flux that is influenced by the southward flowing West Indian Coastal Current (WICC). During the Fall inter-monsoon (Figure 1c), the spatial extent of the northward flux along the SC is reduced, the southward salt flux along the eastern AS region reverses direction to become northward and the southward flux along the western BoB extends further toward Sri Lanka. The flux in the western BoB is controlled by the southward flowing EICC that, during the NE monsoon season, goes around the Sri Lankan coast carrying with it fresher water into the AS. From December to February during the NE monsoon season northward flux along the eastern AS intensifies and its spatial extent spreads into the central AS (Figure 1d). This flux is under the influence of the WICC. During NE monsoon, the flux is southward along the southern SC and at the equator.

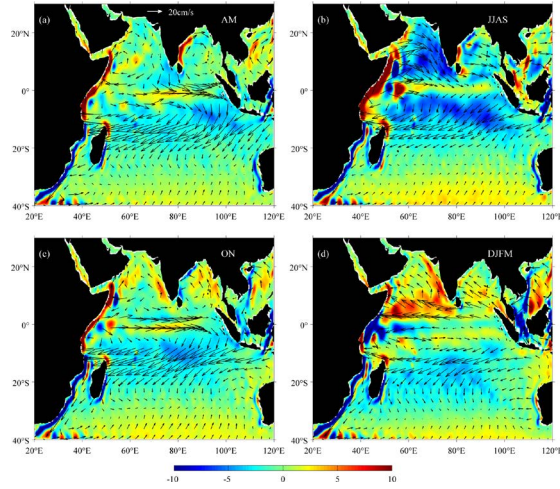


Figure 1. 49-year mean meridional surface salt flux ($\text{kg m}^{-2} \text{s}^{-1}$) overlaid with current vectors for (a) April-May, (b) June, July, August, September, (c) October-November and (d) December, January, February, March (Nyadjro et al., 2013a).

Long-term mean near-surface zonal salt flux (Figure 2) is of higher magnitude than long-term mean near-surface meridional salt flux. The strongest zonal flux of near surface salt occurs northward of 20°S with the most noticeable region being between 5°S and 15°S where salt flux is westward year-round. This band extends eastward from the western boundary and is under the influence of the South Equatorial Current (SEC). The SEC is westward year-round and is driven by the southeast trade winds. The SEC bifurcates with the northward branch forming the Northeast Madagascar Current (NEMC) that feeds into the EACC. The northernmost extent of this westward flux into the EACC is maximum during the SW monsoon (Figure 2b). The impact of Wyrтки jets on salt flux is apparent along the equator during AM (Figure 2b) and ON (Figure 2c). The jets are directly forced by westerly winds and cause the eastward flux of salt along the equatorial region. The zonal salt flux during AM extend further east than during ON. During the SW monsoon season (Figure 2b) salt flux is eastward along the entire central and western AS, Somali coast and western BoB. During the NE monsoon (Figure 2d), the eastward flux that positioned directly above the equator reverses to westward flux with the reversals of currents.

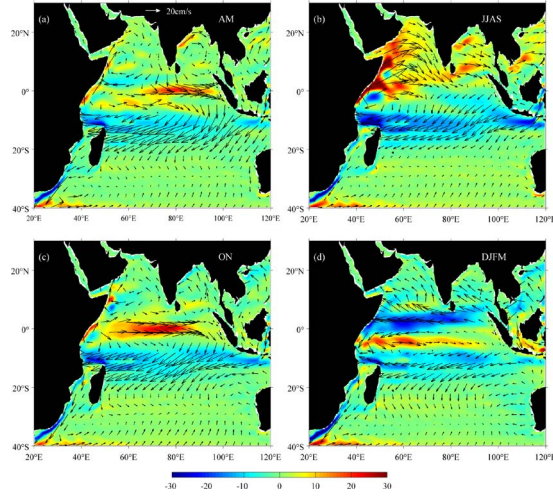


Figure 2. 49-year mean zonal surface salt flux ($\text{kg m}^2 \text{s}^{-1}$) overlaid with current vectors for (a) April-May, (b) June, July, August, September, (c) October-November and (d) December, January, February, March (Nyadjro et al., 2013a).

A preliminary result of salt flux computed from OSCAR currents and Argo SSS (Figure 3a-b), SMOS SSS (Figure 3 c-d) and Aquarius SSS (Figure 3 e-f) for October-November 2011 is presented. The spatial patterns observed in the ON zonal salt flux climatology (Figure 3c) are replicated here (Figure 3a, c, e) with the eastward and westward salt fluxes well captured in the satellite-derived data. Similarly, the meridional salt flux (Figure 3b, d, f) compares favorably well with the ON meridional salt flux climatology (Figure 3c). The northward flux along the northern SC region is however slightly weaker in Aquarius data (Figure 3f) than in Argo (Figure 3b) and SMOS (Figure 3d).

SODA successfully simulates the observed near-surface salt flux in the Indian Ocean. Zonal salt flux is found to be of a higher magnitude than meridional salt flux and it is also influenced more by IOD and ENSO climate modes than meridional salt flux. Salt flux is estimated from changes in salinity and currents and the patterns of the flux also track the patterns of currents in the Indian Ocean. Because surface currents in the Indian Ocean are predominantly wind-driven, changes in wind directions and magnitudes affect surface currents and consequently the salt flux variability.

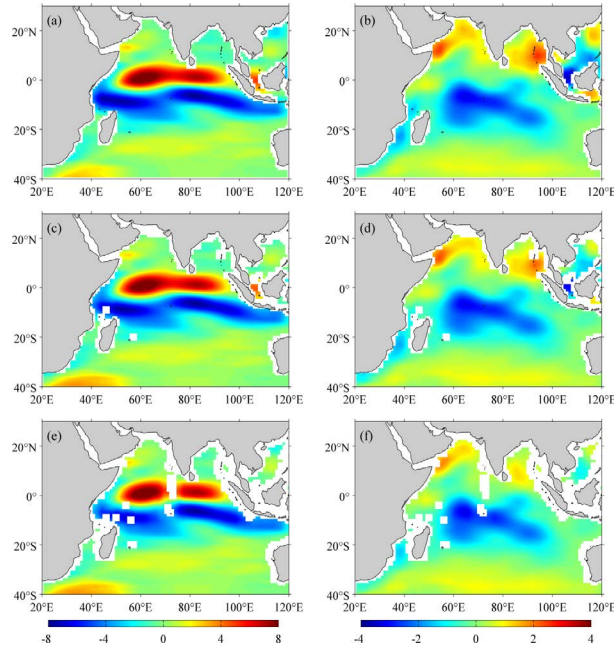


Figure. 3 Mean salt flux ($\text{kg m}^2 \text{s}^{-1}$) for October–November, 2011 computed from OSCAR currents and Argo (a and b), SMOS (c and d) and Aquarius (e and f). Left panel shows zonal salt flux and right panel shows meridional salt flux (Nyadjro et al., 2013a).

A preliminary analysis of results from satellite-derived SSS shows erratic salinity retrievals in the northern Indian Ocean. Salt flux estimates from this are quite promising with the tendency to replicate the results in this study when more satellite-derived SSS data becomes available. Future studies will include the analyses of salt convergence and divergence, which are required to fully link salt changes with salt fluxes. Such studies will involve using the surface fluxes as integration reference points in order to obtain fluxes across depth sections.

2. The role of coastal Kelvin waves on the fresh and salt water transports

Propagation of first upwelling Kelvin Wave and surface circulation (January–March)

In early January (SSHA shows regions of lower-than-average sea level (negative SSHA) in the latitudes along the equatorial Indian Ocean, as well as along the coasts of the Andaman Sea and northern BoB. In the western BoB, the region of low SSHA is likely due to the presence of a cyclonic eddy which commonly occurs in winter. The intense cyclonic eddy in the southeastern BoB in February also weakens by late March.

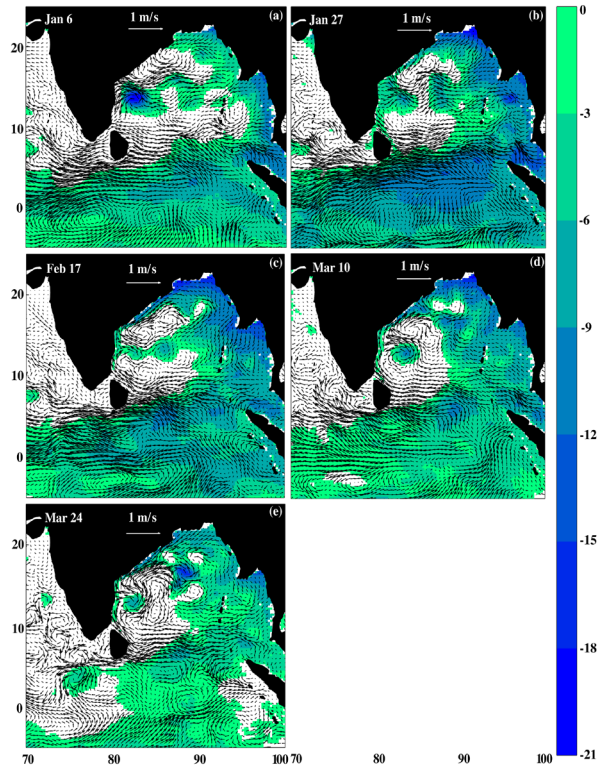


Figure 4: 4 year weekly average sea surface height anomaly (SSHA) from HYCOM in the Indian Ocean, displayed at 2-3 week intervals from January-March. Only negative values of SSHA are displayed to show the propagation of the first upwelling Kelvin wave. Overlaid are the weekly averaged absolute sea surface current vectors calculated using U and V from HYCOM (Nienhaus et al., 2012).

Propagation of first downwelling Kelvin Wave and surface circulation (April - June)

By April (Figure 5) the downwelling equatorial Kelvin wave has reached the Sumatra coast and has begun flowing into the Andaman Sea. Surface currents are now following the propagation of the downwelling wave, and are steadily increasing in magnitude. The large anticyclonic gyre persists through April in the center of the BoB, with the core clearly off the Indian coast in the southwestern BoB. This anticyclonic gyre is generated due to the propagation of the first upwelling Kelvin wave as seen in Figure 4.

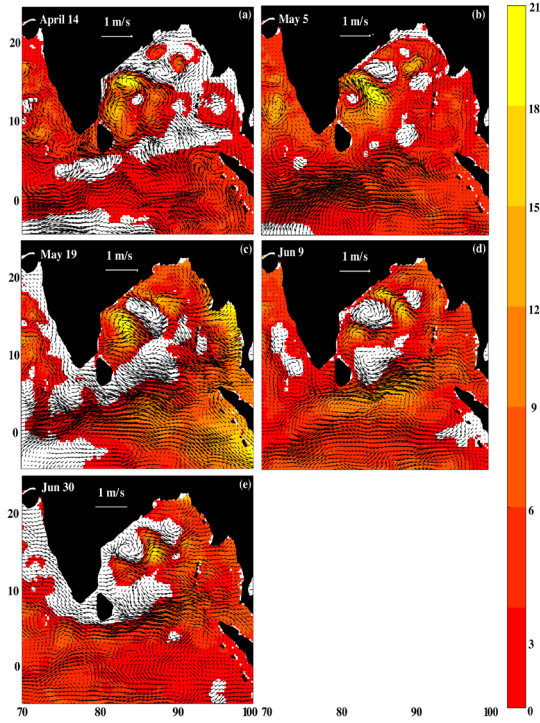


Figure 5: 4 year weekly average sea surface height anomaly (SSHA) from HYCOM in the Indian Ocean, measured at 2-3 week intervals from April-June. Only positive values of SSHA are displayed to show the propagation of the first downwelling Kelvin wave. Overlaid are the weekly averaged absolute sea surface current vectors calculated using U and V from HYCOM (Nienhaus et al., 2012).

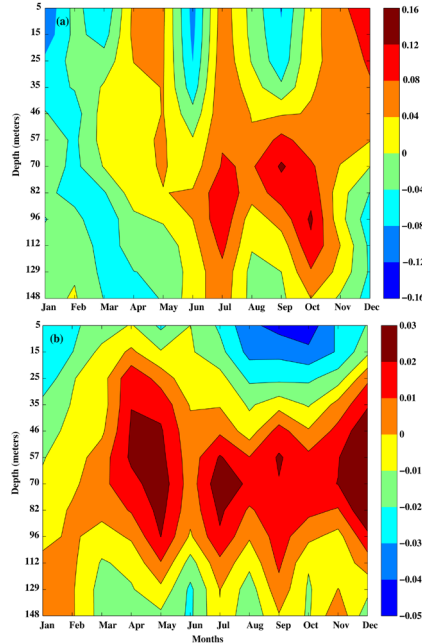


Figure 6. Time series of (a) zonal (U) current velocity anomalies (m/s) averaged from SODA reanalysis at 0°N , 77°E (south of India on equator) and (b) alongshore current velocity (V) anomalies (m/s) averaged from SODA reanalysis at 2°N , 94°E (near Sumatra coast) over the period from 1993-2006. The top 12 layers of SODA reanalysis correspond to a depth of about 148 m (Nienhaus et al., 2012).

At 0°N, 77°E, zonal velocity (U, Figure 6a) ranges from -0.16 m/s to +0.16 m/s. The westward (negative) zonal velocity in January, boreal winter season, is a manifestation of the first upwelling Kelvin wave, followed by the first downwelling (eastward, positive zonal velocity) in April/May, the second upwelling Kelvin wave in August-September. The second downwelling Kelvin wave first appears at the thermocline during September-October and then progresses towards the surface by November-December and is stronger than the first downwelling Kelvin wave. Similarly, the alongshore current velocity at 2°N, 94°E (off northern Sumatra, Figure 6b) also shows the first and second downwelling Kelvin waves associated with the northward (positive) alongshore velocity anomaly during April-May and October-December at thermocline depths. The alongshore southward velocity associated with the first and second upwelling Kelvin waves is weaker and limited to shallow layer only. These coastal Kelvin waves have a propagating horizontal speed of ~2.5 m/s and a vertical speed of ~1.2 m/day.

3. The salinity structure of the Indian Ocean Dipole

The importance of Indian Ocean dynamics to the regional and global ocean-climate signatures is increasingly recognized at large partly due to improved ocean observations in the recent few years. A key component of better understanding the region is the resolving of salinity variability within a dynamic freshwater flux environment. The freshwater influx leads to intense salinity stratification and helps maintain warmer surface temperature. The current provision of satellite-measured, spatially dense SSS data have enhanced the study of oceanic processes that demand the inclusion of salinity data. In this study, we presented results of the salinity structure of the Indian Ocean as captured from the SMOS satellite.

Figure 7 shows the variability of Sea Surface Salinity (SSS) from Soil Moisture and Ocean Salinity (SMOS0 mission. During the 2010 negative Dipole, N-IOD, (Figure 7a-c), SMOS was able to capture low salinity waters around Java and southern Sumatra coastal regions (JSC, smaller box in Figure 7a-c; 4°S-11°S, 99°E-114°E). This low SSS at this location was absent during 2011 (Figure 7d-f). There is also anomalously low SSS waters advected equatorward from the Bay of Bengal (Figure 7a-c). SMOS was also able to capture anomalously high SSS along the south-central Indian Ocean region (SCIO, bigger box in Figure 7a-c; 1°S-9°S, 65°E-98°E). This SSS structure was absent during 2011 (Figure 7d-f). Temporal evolution of box-averaged anomalous SSS in JSC shows the lowest SSS was observed between September and November 2010, during the peak of the N-IOD event (Figure 7g). During the same time periods in 2011 and 2012, the anomalous SSS was relatively higher. Conversely, higher anomalous SSS was observed in the SCIO region (Figure 7h). During the same time periods in 2011 and 2012, anomalous SSS was relatively lower.

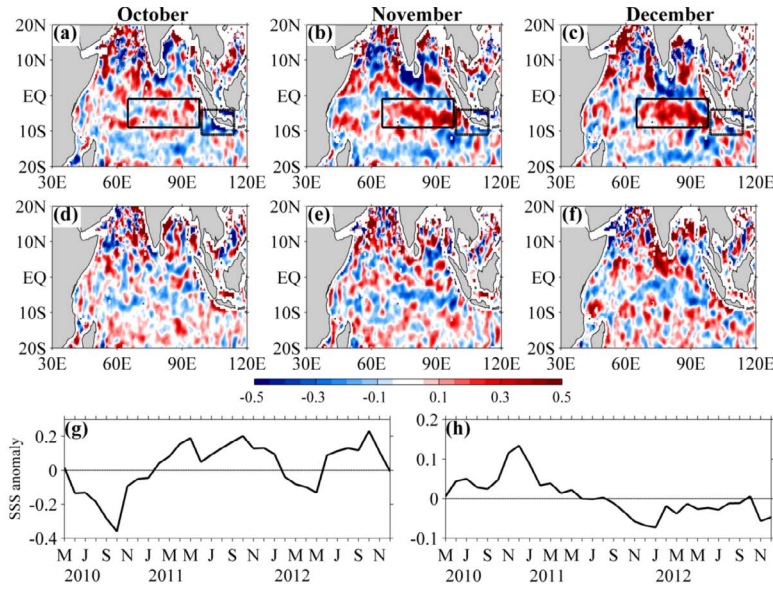


Figure 7. Sea surface salinity (SSS) anomalies for (top row) 2010 and (middle row) 2011 for (a, d) October, (b, e) November and (c, f) December. (g) SSS anomalies for May 2010–December 2012 for the smaller box in (a–c), JSC region. (h) SSS anomalies for May 2010–December 2012 for the bigger box in (a–c), SCIO. Anomalies are computed as monthly data minus monthly climatology (Nyadjro et al., 2013b).

The provision of extensive SSS data have aided the computation of the salt budget terms from SMOS for the first time in the Indian Ocean. It is shown that SMOS is able to resolve the observed SSS pattern in the Indian Ocean with key challenges being in the northern Indian Ocean mainly as a result of radio frequency interferences and ocean-land contamination. During the 2010 N-IOD event, anomalously high SSS waters were observed in the SCIO region (Figure 7) mainly due to the flux of high saline waters from the northwestern Indian Ocean (Figure 8), advection of high saline sub-surface waters as well as reduced precipitation. Conversely in the JSC region, SSS was anomalously lower despite the eastward salt flux into the region. The SSS variability here was driven more by precipitation exceeding evaporation in September–October 2010. This lowered SSS, aided the creation of salinity stratification that strengthened the barrier layer during this period than comparable periods in 2011 and 2012, and suppressed the advection of high saline sub-surface waters into the surface region. The results show that in future more SSS data from SMOS and Aquarius satellites will enhance our understanding of air-ocean coupled processes in the Indian Ocean.

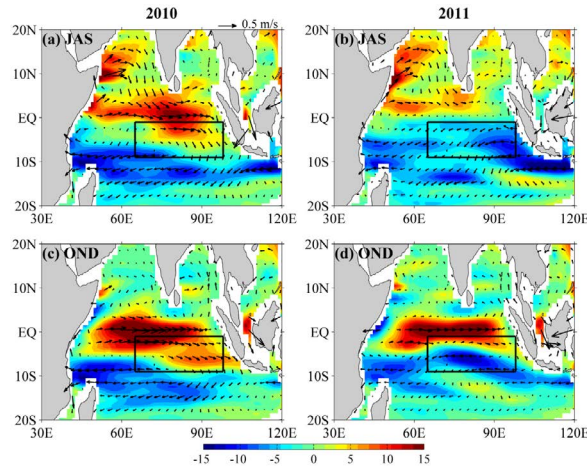


Figure 8. Salt flux ($\text{kg m}^2 \text{s}^{-1}$) for (left panel) 2010 and (right panel) 2011 for (a, b) July-September and (c, d) October-December. Arrows show OSCAR currents (Nyadjro et al., 2013b).

IMPACT/APPLICATIONS

For Naval applications, understanding salinity transport in the Indian Ocean is relevant in the area of anti-submarine warfare. Salinity transport impacts density fronts and the depth of both the mixed layer and thermocline, which are important for acoustic performance predictions. The regions like the Bay of Bengal where freshwater occupies the top layer, the sound velocity profile will change and there will be acoustic losses. Internal waves can be generated due to the strong salinity stratification, and barrier layer formation occurs. Also, investigations on the ocean transport processes and their effects on the carbon flux fall within ONR's quest to understand "environmental evolution, assimilation of data, and the limits of predictability by planning, fostering and encouraging scientific inquiry and technological development in fields ranging from littoral geosciences to high latitude dynamics."

RELATED PROJECTS

None

PUBLICATIONS

- **Refereed Publications**

1. Nyadjro, E.S, and B. Subrahmanyam (2013b). SMOS salinity mission reveals salinity structure of the Indian Ocean Dipole, IEEE Geoscience and Remote Sensing Letters, (in review).
2. Felton, C., Subrahmanyam, B., V.S.N. Murty (2013). ENSO Modulated cyclogenesis over the Bay of Bengal, Journal of Climate (in press).
3. Nyadjro, E.S., and B. Subrahmanyam, and B.S. Giese (2013a). Variability of Salt flux in the Indian Ocean during 1960-2008, Remote Sensing of Environment, 134, 175-193.

4. Nienhaus, M.S., and B. Subrahmanyam, and V.S.N. Murty (2012). Altimetric Observations and Model simulations of Coastal Kelvin Waves in the Bay of Bengal, OSTM/Jason-2 special issue, Marine Geodesy , Volume 35, Supplement 1, 190-216, 2012.

- ***Conference/Workshop presentations***

1. **Subrahmanyam, B. (2013).** Validation of Aquarius and SMOS salinity measurements in the Indian Ocean, 15-17 April 2013, IFREMER, Brest, France (*Invited Presentation*).
2. Button, N., **B. Subrahmanyam** (2013). Validation of SMOS and Aquarius Salinity data in the Agulhas region, 15-17 April 2013, IFREMER, Brest, France (*Invited Presentation*).
3. **Subrahmanyam, B.,** E.S. Nyadjro, G. Grunseich (2012). Preliminary Aquarius and SMOS salinity measurements validation in the Indian Ocean, Fall AGU Meeting, San Francisco, 3-7 December 2012 (*Poster Presentation*).
4. E.S. Nydjro, **B. Subrahmanyam** (2012). Variability of salt transport in the Indian Ocean, Fall AGU Meeting, San Francisco, 3-7 December 2012 (*Oral Presentation*).
5. Nyadjro, E.S., **B. Subrahmanyam** (2012). Variability of Salt Transports in the Indian Ocean, Fall AGU Meeting, San Francisco, 3-7 December 2012 (*Oral Presentation*).

HONORS/AWARDS/PRIZES

1. Dr. Subrahmanyam Bulusu (PI) was named one of USC's **2013 Breakthrough Rising Stars** by the Office of Research, University of South Carolina.
2. Dr. Subrahmanyam Bulusu's article, [*Mapping Sea Salt From Orbit: Building Better Ocean and Climate Models*](#), featured in **Science Daily**!